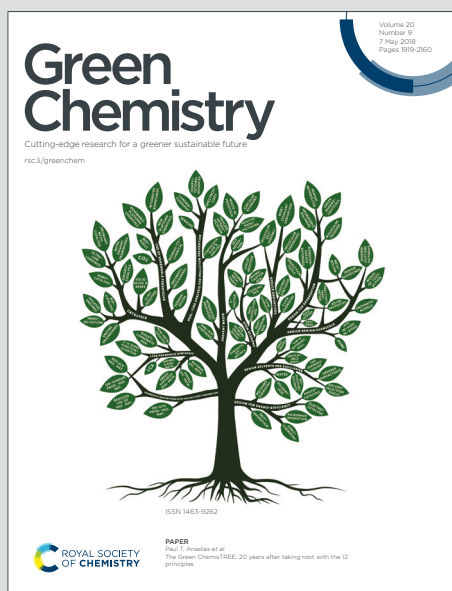


# Green Chemistry

Cutting-edge research for a greener sustainable future

Accepted Manuscript

This article can be cited before page numbers have been issued, to do this please use: G. Lu, X. Li, L. Zhong, S. Li and F. Chen, *Green Chem.*, 2019, DOI: 10.1039/C9GC02181G.



This is an Accepted Manuscript, which has been through the Royal Society of Chemistry peer review process and has been accepted for publication.

Accepted Manuscripts are published online shortly after acceptance, before technical editing, formatting and proof reading. Using this free service, authors can make their results available to the community, in citable form, before we publish the edited article. We will replace this Accepted Manuscript with the edited and formatted Advance Article as soon as it is available.

You can find more information about Accepted Manuscripts in the [Information for Authors](#).

Please note that technical editing may introduce minor changes to the text and/or graphics, which may alter content. The journal's standard [Terms & Conditions](#) and the [Ethical guidelines](#) still apply. In no event shall the Royal Society of Chemistry be held responsible for any errors or omissions in this Accepted Manuscript or any consequences arising from the use of any information it contains.

## ARTICLE

**Ru@UiO-66(Ce) Catalyzed Acceptorless Dehydrogenation of Primary Amines to Nitriles: The Roles of Lewis Acid-base pairs on the Reaction***Guo-Ping Lu,<sup>a,b,\*</sup>, Xinxin Li,<sup>a+</sup> Lixiang Zhong,<sup>b</sup> Shuzhou Li<sup>b</sup> and Fei Chen<sup>c</sup>*Received 00th January 20xx,  
Accepted 00th January 20xx

DOI: 10.1039/x0xx00000x

UiO-66(Ce)-encapsulated ruthenium nanoparticles (Ru@UiO-66(Ce)) was designed and used for dehydrogenation of primary amines to nitriles in water without any hydrogen acceptor and additives. Introduction of metal Ru to UiO-66(Ce) contributes to the formation of Lewis acid-base pair [Ru-O-Ce-Vö] on catalyst owing to the metal-support interaction, acting as active sites for activation of amine and transfer of hydrogen. Ab initio calculation results further confirm the roles of Lewis acid-base pairs in the reaction.

**Introduction**

Nitriles are an crucial class of fundamental organic compounds with a wide applications in natural products,<sup>1</sup> bioactive molecules,<sup>2</sup> industrial processes (polymers, agrochemicals, and dyes/pigments)<sup>3</sup> and serve as versatile intermediates for further synthesis of amides, acids and heterocycles.<sup>4-7</sup> The classical methodologies for nitrile synthesis include Sandmeyer-type reactivity,<sup>8</sup> cyanation of alkyl or aryl halides,<sup>6</sup> dehydration of amides/aldoximes,<sup>12,13</sup> and metal-catalyzed cyanation/cyanomethyl-ation,<sup>14,15</sup> among others.<sup>16-21</sup> However, these conventional methods were often limited by low atom economy, poor reactivity, toxic solvents, drastic reaction conditions. Another methodology is transition-metal-catalyzed conversion of primary amines to nitriles. In general, the use of stoichiometric oxidants as the hydrogen acceptors is norm,<sup>22-25</sup> resulting in low atom economy, disappointing selectivity and bad functional group tolerance.

More recently, transition-metal-catalyzed acceptorless double dehydrogenation of primary amines has been developed, which is a highly desirable, atom-economical route to nitriles, and the evolved hydrogen gas in this process is valuable as a source of clear energy.<sup>26-31</sup> Although some of these processes can be achieved under relatively mild conditions with high selectivity and broad substrate scope,<sup>27,28</sup> they still suffer from limitations including the use of expensive,

pre-prepared and unrecoverable ruthenium complex, toxic and flammable organic solvents. Therefore, it is desirable and appealing to explore innovative heterogeneous catalysts for the transformation in greener solvents, which also meets the principle of green chemistry.<sup>32-34</sup>

On the other hand, Wang's group reported that Ru/ceria with rich oxygen vacancy (Vö) content could form the interfacial Lewis acid-base pair [Ru-O-Ce-Vö] that acts as active site for the dissociation of methanol or amines and the subsequent transfer of hydrogen to the activated alkenes or CO.<sup>35-37</sup> Inspired by above-mentioned reports, we come up with an innovative idea that Lewis acid-base pair [Ru-O-Ce-Vö] contains acidic Ce-Vö site and basic interfacial oxygen of Ru-O-Ce linkage, may act as active sites for the absorption and activation of amines and the transfer of hydrogen to Ru to produce H<sub>2</sub>.<sup>38</sup> Compared with CeO<sub>2</sub>, UiO-66(Ce) as a porous material with higher surface areas also has cerium-oxygen clusters that may be more easily to form oxygen vacancies due to its unstable structure under reduction conditions.<sup>39-41</sup>

Researches on Ru/CeO<sub>2</sub> are uninterrupted,<sup>35-37,42-46</sup> but the study of Ru/UiO-66(Ce) is still blank. In view of the properties of UiO-66(Ce), we believe that the combination of Ru and UiO-66(Ce) may bring more possibilities for catalyst development. Based on these results, we reason that (1) the uniform and small cavities of UiO-66(Ce) may restrict the growth of Ru NPs and afford more active metal sites;<sup>47-51</sup> (2) the introduction of metal Ru to UiO-66(Ce) may contribute to the formation of Lewis acid-base pairs [Ru-O-Ce-Vö] due to the metal-support interaction between Ru and UiO-66(Ce),<sup>35-37,42</sup> which can enhance the acceptorless double dehydrogenation of primary amines.

**Results and discussion**

<sup>a</sup> School of Chemical Engineering, Nanjing University of Science & Technology, Xiaolingwei 200, Nanjing 210094, P. R. China. glu@njut.edu.cn

<sup>b</sup> School of Materials Science & Engineering, Nanyang Technological University, 50 Nanyang Avenue, Singapore 639798

<sup>c</sup> Nanjing Institute of Environmental Sciences, Ministry of Ecology and Environment, Nanjing, 210042, China

\* These authors are contributed equally to this paper.

Electronic Supplementary Information (ESI) available. See DOI: 10.1039/x0xx00000x

**Table 1** Optimization of reaction conditions<sup>a</sup>

Entry	Catalyst	Solvent	Yield (%) <sup>b</sup>
1	Pd@UiO-66(Ce)	toluene	6
2	Pt@UiO-66(Ce)	toluene	nr
3	Ru@UiO-66(Ce)	toluene	29
4	Ru@UiO-66(Ce)	MeOH	6
5	Ru@UiO-66(Ce)	EtOH	nr
6	Ru@UiO-66(Ce)	MeCN	5
7	Ru@UiO-66(Ce)	acetone	nr
8	Ru@UiO-66(Ce)	DMSO	65
9	Ru@UiO-66(Ce)	H <sub>2</sub> O	72
10	Ru <sub>1</sub> Nb <sub>1</sub> @UiO-66(Ce)	H <sub>2</sub> O	50
11	Ru <sub>1</sub> Nb <sub>3</sub> @UiO-66(Ce)	H <sub>2</sub> O	57
12	Ru <sub>1</sub> Nb <sub>5</sub> @UiO-66(Ce)	H <sub>2</sub> O	54
13	Ru <sub>1</sub> Ni <sub>1</sub> @UiO-66(Ce)	H <sub>2</sub> O	63
14	Ru <sub>1</sub> Ni <sub>3</sub> @UiO-66(Ce)	H <sub>2</sub> O	58
15	Ru@UiO-66(Zr)	H <sub>2</sub> O	33
16	Ru@MIL-125(Ti)	H <sub>2</sub> O	27
17	Ru@Mg-MOF-74	H <sub>2</sub> O	36
18	Ru@MIL-101(Fe)	H <sub>2</sub> O	35
19	Ru@CeO <sub>2</sub>	H <sub>2</sub> O	58
20	Ru NPs	H <sub>2</sub> O	26
21	UiO-66(Ce)	H <sub>2</sub> O	trace
22	UiO-66(Ce)-NaBH <sub>4</sub> <sup>c</sup>	H <sub>2</sub> O	nr
23	Ru@UiO-66(Ce)	H <sub>2</sub> O	75 <sup>d</sup>
24	Ru@UiO-66(Ce)	H <sub>2</sub> O	53 <sup>e</sup>

<sup>a</sup> Conditions: dodecylamine (0.2 mmol), catalyst amount (1 mol%) was measured based on Ru, solvent (1 mL), stirred in a sealed tube at 130 °C under N<sub>2</sub> atmosphere for 16 h. <sup>b</sup> The yields were determined by GC using biphenyl as the internal standard. <sup>c</sup> UiO-66(Ce)-NaBH<sub>4</sub> was derived from the reaction of NaBH<sub>4</sub> and UiO-66(Ce). <sup>d</sup> The catalyst amount was 2 mol%. <sup>e</sup> The catalyst amount was 0.5 mol%.

To verify the feasibility of our proposed assumption, we started the investigation by choosing the dehydrogenation of dodecylamine to dodeconitrile liberating clean hydrogen gas as a model reaction. Initial, trace of dehydrogenated product (6 %) was achieved after 16 h when using 1 mol% Pd@UiO-66(Ce) as the catalyst in toluene at 130 °C (Table 1, entry 1) and even monometallic Pt did not possess catalytic efficiency (entry 2). A slightly meaningful transformation of 29% dodecylamine to dodeconitrile was appeared when using Ru@UiO-66(Ce) as the catalyst (entry 3). To further improve the unsatisfactory yield, different solvents were screened. Several polar solvents afforded unsatisfactory results (entries 4-7) while the delightful conversions of dodecylamine to dodeconitrile in DMSO and H<sub>2</sub>O (entries 8, 9) due to the better dissolution of catalyst in DMSO and H<sub>2</sub>O.

Consistent with “synergistic effects” of bimetallic nanoparticles,<sup>55-57</sup> Ru alloy with Nb or Ni were tried, but no obvious enhancement on catalytic performance was observed (entries 10-14). Other MOFs were employed as the carriers, but all of them showed lower catalytic activity (entries 15-18). As expected, dodeconitrile was obtained in a moderate yield employing Ru@CeO<sub>2</sub> as the catalyst, and illustrating that Lewis

acid-base pairs [Ru-O-Ce-Vö] might play an important role in this reaction.<sup>35-37</sup> Considering the contribution of immobilized metal and support, unsupported Ru NPs was also attempted in this reaction. The poor catalytic performance could be a result of serious agglomeration of the Ru NPs during the reaction process and the lack of Lewis acid-base pairs (entry 20). In addition, UiO-66(Ce) and UiO-66(Ce)-NaBH<sub>4</sub> failed to yield the desired products (entries 21, 22), indicating that Ru species were the main active sites for the dehydrogenation reaction. Furthermore, there was no obvious differences on reaction yield increasing catalyst amount to 2 mol% (entry 23), but lowering the catalyst amount to 0.5 mol% caused visible decrease in yield (entry 24). No side reaction was observed in all cases. The remained starting material **1a** after these reactions resulted to the low to moderate yields of **2a**.

To further confirm the presence of oxygen vacancy (Vö) and Lewis acid-base pairs in Ru@UiO-66(Ce), the catalyst was characterized by Raman spectroscopy. The Raman spectra indicate the presence of rich Vö on both UiO-66(Ce)-NaBH<sub>4</sub> and Ru@UiO-66(Ce) in comparison of pristine UiO-66(Ce) (Fig. 1). A main band centered at 463 cm<sup>-1</sup> assigns to the F<sub>2g</sub> vibrational mode of UiO-66(Ce).<sup>58</sup> For the UiO-66(Ce)-NaBH<sub>4</sub> and Ru@UiO-66(Ce), the peaks assigned to F<sub>2g</sub> vibrational mode still remain but blue-shifted and broadened compared with UiO-66(Ce). This may be due to the presence of oxygen vacancies derived under reduction conditions<sup>59,60</sup> or the introduction of Ru into the UiO-66(Ce).<sup>42,61</sup> Both oxygen vacancies and the introduction of Ru into the UiO-66(Ce) can change the structure of UiO-66(Ce), thus leading to the alteration of F<sub>2g</sub> vibrational frequency and mode (the blue-shifted and broadened peak). Two peaks at 695 cm<sup>-1</sup> and 975 cm<sup>-1</sup> are also observed on Ru@UiO-66(Ce), which are assigned to the existence of Ru-O-Ce or Ru=O stretching.<sup>36</sup>

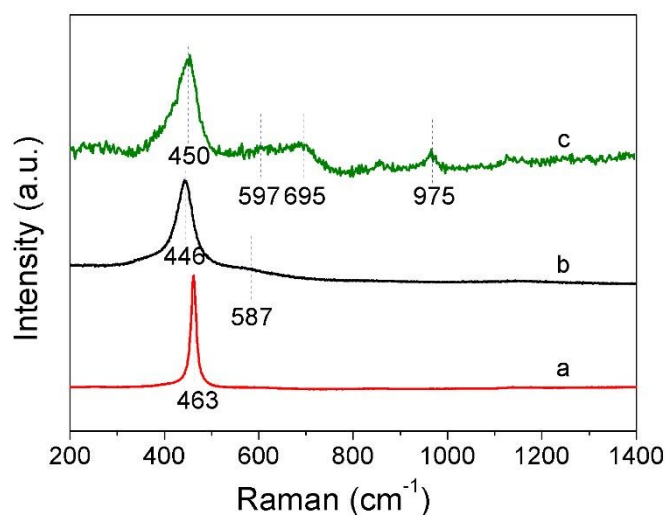


**Fig. 1** Raman spectra of (a) UiO-66(Ce) (b) UiO-66(Ce)-NaBH<sub>4</sub> (c) Ru@UiO-66(Ce).

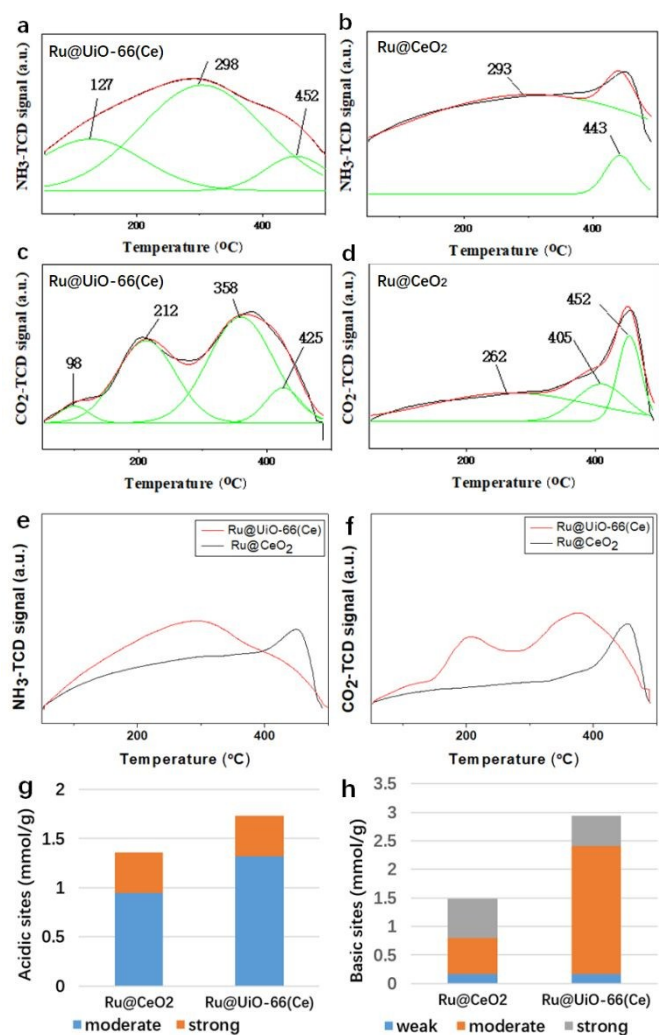


**Fig. 2** (a), (b), (e) NH<sub>3</sub>-TPD profile; (c), (d), (f) CO<sub>2</sub>-TPD profile; the number of (c) acidic sites and (d) basic sites of Ru@UiO-66(Ce) and Ru@CeO<sub>2</sub>.

In order to further determine the acid-base properties of Ru@UiO-66(Ce), NH<sub>3</sub>-temperature-programmed desorption (NH<sub>3</sub>-TPD) and CO<sub>2</sub>-TPD were tested. As Fig. 2a, 2b, 2e, 2g shown, two main kinds of acid sites belong to Ru@UiO-66(Ce) and Ru@CeO<sub>2</sub> on similar positions. The number of strong acid sites (> 400 °C) of Ru@UiO-66(Ce) is similar with Ru@CeO<sub>2</sub>, but the number of moderate acid sites (200 °C-400 °C)<sup>62</sup> of Ru@UiO-66 is more than Ru@CeO<sub>2</sub> (Fig. 2g). Base properties of Ru@UiO-66(Ce) are demonstrated on Fig. 2c, four peaks are recorded which are assigned to three kinds of base sites: strong basic sites at 452 °C, moderate basic sites at 358 °C and 212 °C and weak basic (<200 °C) sites at 98 °C. Compared with Ru/CeO<sub>2</sub>, Ru@UiO-66(Ce) has much more moderate basic sites but less strong basic sites (Fig. 2c, 2d, 2f, 2h). The dates suggest that Ru@UiO-66(Ce) is an acid-base catalyst, and more acidic and basic sites means more Lewis acid-base pairs, thus leading to better catalytic activity considering the fact that Ru@UiO-66(Ce) catalysed reaction provides a better yield than Ru@CeO<sub>2</sub>.

No obvious XRD single of Ru@UiO-66(Ce) and UiO-66(Ce)-NaBH<sub>4</sub> is detected after the treatment of NaBH<sub>4</sub> (Fig. S1),

indicating that the crystal structure of UiO-66(Ce) has been destroyed. The sharp reduction BET surface area of Ru@UiO-66 compared with UiO-66(Ce) (251 m<sup>2</sup>/g vs 919 m<sup>2</sup>/g in Table S1) are also agree with the results of XRD. However, Ru@UiO-66 still has much better BET surface area than Ru@CeO<sub>2</sub> (251 m<sup>2</sup>/g vs 35 m<sup>2</sup>/g). Based on the results of scanning electron microscope (SEM) and transmission electron microscopy (TEM) measurements (Fig. 3), similar size but more irregular particles is observed compared with the features of UiO-66(Ce),<sup>39-41</sup> which is also consistent with the results of XRD and BET. No clear Ru NPs can be observed due to the low laden quantity of metal Ru in UiO-66(Ce) which results in small diameter Ru NPs. Therefore, inductively coupled plasma mass spectrometry (ICP-MS) was adopted to determine the amount of Ru in the Ru/UiO-66(Ce), the load data 0.8 wt% confirmed the above conjecture (Table S1).

To determine the distribution of Ru species on this catalyst, the representative high-resolution TEM (HRTEM) image are shown in Fig. 3d, unobvious Ru lattice fringes (red circles) on catalyst were detected, suggesting that the Ru sizes are tiny and Ru species are highly dispersed in support. The ultrafine Ru NPs and highly dispersed distribution provide more active metal atoms and more contact opportunities between the active sites and substrates, leading to higher catalytic efficiency. Furthermore, TEM-EDS mapping of Ru@UiO-66(Ce) was applied (Fig. 6). The images distinctly display the existence of Ru in the catalyst (Fig. 4).

The XPS measurement unraveled the details about surface composition and chemical states of Ru@UiO-66(Ce). The overall survey of catalyst clearly shows the Ce, O, C and Ru element signals. There occur positions overlap of C and Ru signals (Fig. 5a). The XPS spectra in the O 1s region can be deconvoluted into three different peaks (Fig. 5b). The peaks at the binding energy about 529.9 eV and 513.1 eV arise from the surface lattice oxygen specie (O<sub>L</sub>) and defect oxides (O<sub>D</sub>) respectively, and oxygen components in the BTC linkers may with the binding energy of 532.0 eV.<sup>61</sup> The signal of Ru 3d<sub>5/2</sub> (282.2 eV) is often used for analyzing the charge state of the Ru species because another signal of Ru 3d<sub>3/2</sub> overlaps with C 1s at around 284.6 eV (Fig. 5c).<sup>36,63,64</sup> The peak at binding energy of 282.2 eV is assigned to the high valence state of RuO<sub>2</sub> 3d<sub>5/2</sub>, owing to surface oxidized of Ru(0) when exposed to air at ambient temperature.<sup>36</sup> The peak at binding energies of 285.8 eV is assigned to Ru(0)<sup>65</sup> and the binding energy 289.2 eV belongs to C of the carboxyl group.<sup>66</sup>

The XPS spectra of Ce 3d can be deconvoluted into eight different peaks from four pairs of spin-orbit doublets (Fig. 7d). The peaks of 3d<sub>5/2</sub> level of Ce<sup>4+</sup> are tagged as v (882.0 eV), v' (888.4 eV) and v'' (897.9 eV) respectively, moreover the peaks labelled as u (900.4 eV), u'' (906.5 eV) and u''' (916.4 eV) are ascribed to 3d<sub>3/2</sub> level of Ce<sup>4+</sup>. The two possible electron configurations of the eventual state of Ce<sup>3+</sup> species are marked as v' (884.5 eV) and u'(903.0 eV),<sup>67</sup> implying the process of reducing metal precursor following the reduction from Ce<sup>4+</sup> to Ce<sup>3+</sup>.

The XPS spectrums of three MOF materials after the treatment of NaBH<sub>4</sub> were also provided (Fig. S3). All of these

metal species (Fe, Ti, Zr) that build up MOFs only possess one kind of valence state, verifying that there are no changes of

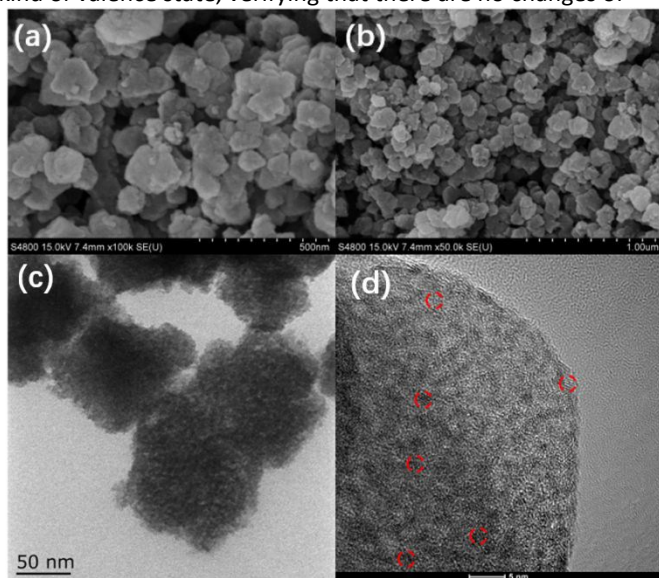


Fig. 3 (a), (b) SEM images of Ru@UiO-66(Ce); (c) TEM image of Ru@UiO-66(Ce); (d) HRTEM image of Ru@UiO-66(Ce) catalyst.

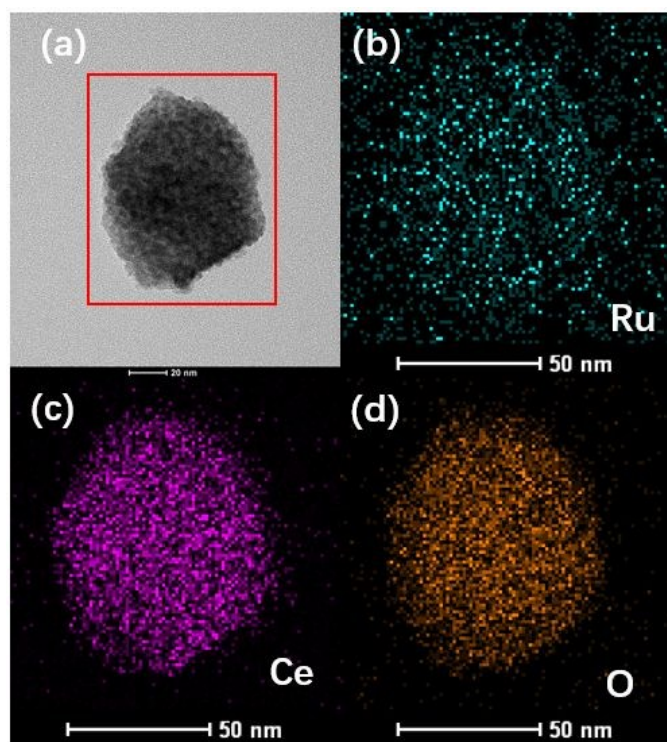


Fig. 4 TEM-EDS mapping images of Ru@UiO-66(Ce) catalyst.

metal sites valence states in MOFs during the reduction process of preparation catalysts. Therefore, oxygen vacancies only exist in Ru@UiO-66(Ce) among all Ru@MOF materials, which may be a main factor for the higher catalytic activity of Ru@UiO-66(Ce) than other Ru@MOFs (Table 1).

The subsequent work turned to establish the scope and generality of this reaction (Scheme 1). Alkyl primary amines with different numbers of carbon atoms was effectively transformed into corresponding long-chain alkyl nitriles under

optimized conditions in moderate to good yields (**2a-2d**). Dehydrogenation of benzylamine gave a poor yield of **2e**, but its derivatives with electron-rich substituent afforded better conversions to corresponding products (**2f-2i**). 4-Chlorobenzylamine still worked in the reaction to yield the desired product **2j**. Benzyl cyanide **2k** could be gained from phenylethylamine with decent yield. *cis*-1-Amino-9-octadecene also converted to corresponding nitrile with a good yield. The dehydration of tetrahydroquinoline was also tried under optimized conditions, and a 75% yield of quinolone **4** was obtained.

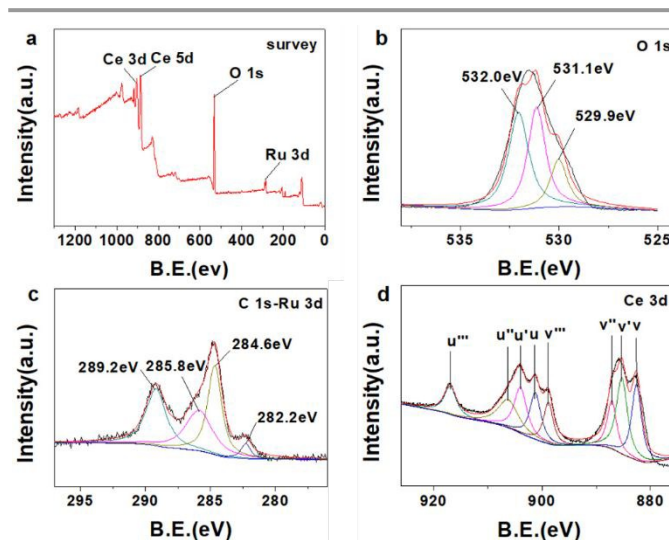
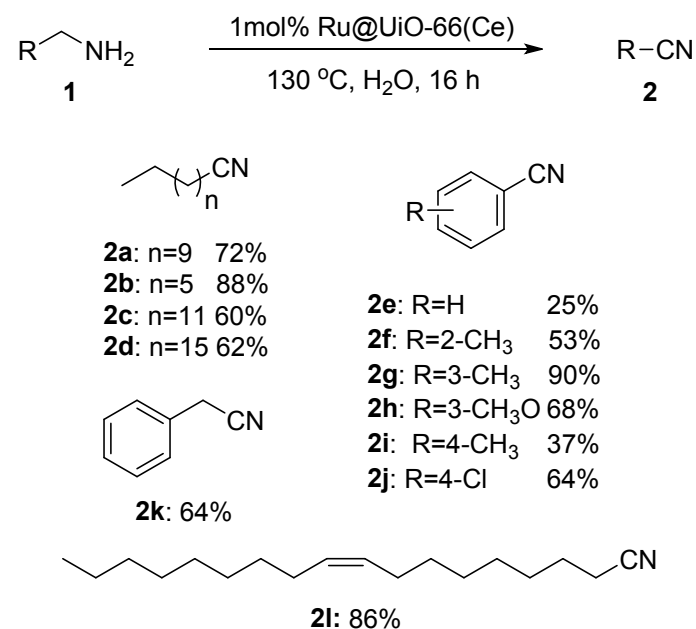
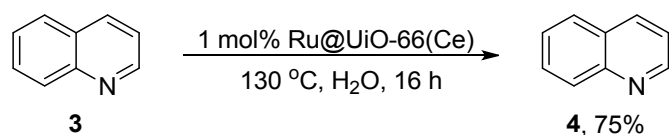
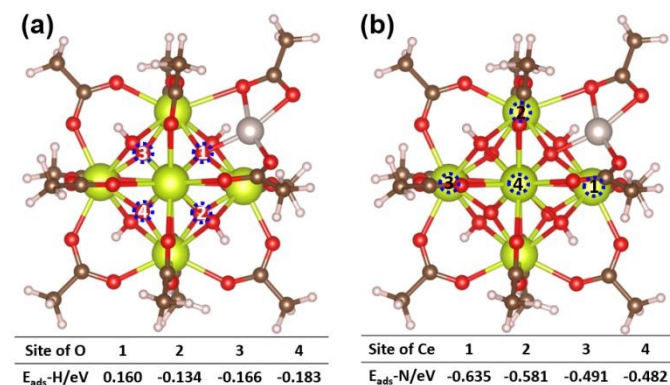


Fig. 5 XPS patterns of Ru@UiO-66(Ce): (a) survey spectrum; (b) high resolution of O spectrum; (c) high resolution of C and Ru spectrum; (d) high resolution of Ce spectrum.





**Scheme 1** The double dehydrogenation of various primary amines catalyzed by Ru@UiO-66(Ce). Conditions: primary amine 0.4 mmol, Ru@UiO-66(Ce) 1 mol%, H<sub>2</sub>O 2 mL, 130 °C, N<sub>2</sub>, 16 h.



**Fig. 6** (a) The adsorption energies of hydrogen on different oxygen sites of Ru@UiO-66(Ce); (b) The adsorption energies of *n*-propylamine on different Ce sites of Ru@UiO-66(Ce). Yellow is Ce; red is O; brown is C; silver is Ru; light gray is H.

To further demonstrate the roles of Lewis acid-base pairs, the adsorption energies of hydrogen on different oxygen sites and amine on different Ce sites were calculated (Fig. 6, S8, S9). As shown in Fig. 6, the introduction of Ru atom into the second building unit of UiO-66(Ce) can form Lewis acid-base pairs [Ru-O-Ce-Vö], because Ru is coordinated with O that used to combine with Ce. The results indicate that the adsorption energy for hydrogen on Ce of [Ru-O-Ce-Vö] (site 1) is 0.160 eV,<sup>68</sup> which is the weakest binding between hydrogen and oxygen among the four types of oxygen sites (Fig. 6a), thus making the transfer of hydrogen located at O of [Ru-O-Ce-Vö] to Ru feasible. Meanwhile, the adsorption energy for amine on Ce of [Ru-O-Ce-Vö] (site 1) is the highest than other three Ce sites, suggesting that the Lewis acid-base pair can enhance the absorption and activation of amines.

Studies were also conducted to access the potential for recycling the catalyst, and double dehydrogenation of dodecylamine to dodecyl nitrile still as a model reaction. Catalyst was centrifuged from the reaction mixture after completion of the reaction, washed with methanol and water, dried in a drying oven and then reused in new reaction. The catalyst was less efficient after it was reused for four times reaction (Fig. 8). The  $O_{\text{DC}}/O_{\text{L}}$  and  $\text{Ce}^{3+}/\text{Ce}^{4+}$  ratios of Ru@UiO-66(Ce) are decreased after reusing four runs (Table S3), which means the loss of interfacial acid-base pair sites.<sup>42</sup> An obvious decrease of C=O single in C 1s region implies the further structural collapse takes place during the reaction and recycling process (Fig. S4c).

The obvious aggregation and deformation of particles observed by SEM and TEM (Fig. S5) also suggests the structural collapse of the catalyst. Furthermore, the loss of Ru was ignored after recycling four times based on the ICP results

(Table S2). Therefore, the loss of interfacial acid-base pair sites and structural collapse of Ru@UiO-66(Ce) may be the two main factors for the deactivation of this material. Finally, in order to prove the production of H<sub>2</sub>, the produced gas was drawn into a syringe and subjected to GC analysis and the retention time matched with a sample collected from a hydrogen cylinder of 99.9% purity (Fig. S6). Volume of the produced gas was measured on a gas burette setup (Fig. S7).

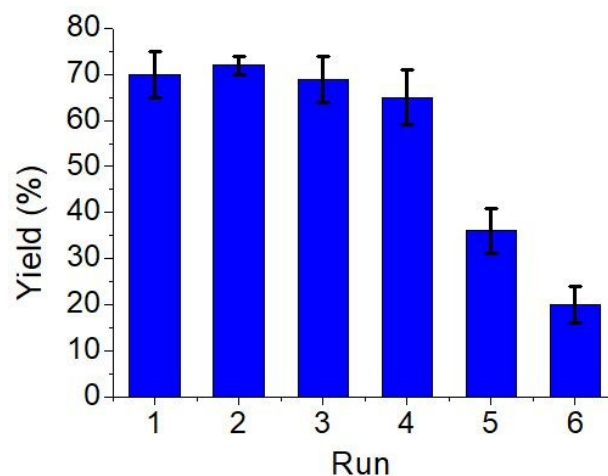


**Fig. 7** Recycle studies. Conditions: dodecylamine 0.4 mmol, Ru@UiO-66(Ce) 1 mol%, H<sub>2</sub>O 2 mL, 130 °C, N<sub>2</sub>, 16 h.

## Experimental

### General

All chemical reagents are obtained from commercial suppliers and used without further purification. GC-MS was performed on an ISQ Trace 1300 in the electron ionization (EI) mode. GC analyses are performed on an Agilent 7890A instrument (Column: Agilent 19091J-413: 30 m × 320 μm × 0.25 μm, carrier gas: H<sub>2</sub>, FID detection). All NMR spectra were recorded on an AVANCE 500 Bruker spectrometer operating at 500 MHz and 126 MHz in CDCl<sub>3</sub>, respectively, and chemical shifts were reported in ppm. The crystal structure of the synthesized catalysts were recorded by X-ray diffraction (XRD) using a D8ADVANCED X-ray diffractometer, employing a scanning rate of 0.1°s<sup>-1</sup>. Scanning electron microscope (SEM) images were taken using a Hitachi S-4800 apparatus on a sample powder previously dried and sputter-coated with a thin layer of gold. Transmission electron microscopy (TEM) images were taken using a PHILIPS Tecnai 12 microscope operating at 120 kv. High Resolution Transmission electron microscopy (HRTEM) was performed on Philips-FEI Tecnai G2 F20 operating at 300kv. X-ray photoelectron spectroscopy (XPS) were performed on a ESCALAB 250Xi spectrometer, using a Al Kα X-ray source (1350 eV of photons). Inductively coupled plasma mass spectrometry (ICP-MS) was analyzed on Optima 7300 DV. Raman spectra were recorded on Aramis with a wavelength of 532 nm. Temperature-programmed desorption (TPD) of NH<sub>3</sub> and CO<sub>2</sub>-TPD were conducted on a Quantachrome TPRWin v3.52 instrument. The samples were

pretreated in He flow at 200 °C with a rate of 15 mL/min for 30 min and cooled to 50 °C, and then swept in CO<sub>2</sub> (NH<sub>3</sub>) flow with a rate of 15 mL/min for 40 min. After treatment in He flow for 50 min to remove physical adsorption, the sample were raised at a heating rate of 10 °C/min to 500 °C, the signals were monitored by a TCD detector. BET surface areas were performed with N<sub>2</sub> adsorption/desorption isotherms at 77 K on a Micromeritics ASAP Tri-star II 3020 instrument. Before measurements, the samples were degassed at 150 °C for 12 h. The generated H<sub>2</sub> gas was detected by a gas chromatograph (Shimadzu GC-2014; Molecular sieve 5A, TCD detector, Ar carrier gas) using a syringe. The Raman spectra were obtained using confocal Raman spectroscopy (inVia-Reflex) employing 785 nm radiation (3 mW).

**The general procedure for the synthesis of MOFs-encapsulated Ru NPs catalysts.** 500 mg support dissolves into 25 mL of water, ultrasonic treatment after metal precursor RuCl<sub>3</sub> (10.3 mg, 0.05 mmol, content of Ru: 5 mg) was added into the mixture, and lysine aqueous solution (0.53 M, 5 mL) was added with vigorous stirring for 4 h at low temperature (< 5 °C). Later, NaBH<sub>4</sub> aqueous solution (0.50 M, 3 mL) was added into suspension liquid dropwise while keeping the temperature below 10 °C. The mixture was continually stirred for 2 h to ensure that metal precursor was completely reduced. Then stop stirring and add acetone (5 mL) keeping for 24 hours. Finally, the catalyst was centrifuged, washed with water and ethanol for three times and dried at 100 °C under vacuum.

**The general procedures for the acceptorless double dehydrogenation of primary amines.** A mixture of primary amine 1 0.2 mmol, Ru@UiO-66(Ce) 1 mol% were added in H<sub>2</sub>O (1 mL), which was stirred under atmospheric N<sub>2</sub> at 130 °C for 16 h. After the reaction was completed, the reaction mixture was extracted by EtOAc (2 mL×2). The obtained organic layer was collected and removed in *vacuo* to afford the crude product 2. Further column chromatography on silica gel was required to afford the pure desired products. The catalyst was centrifuged from the reaction mixture after completion of the reaction, washed with methanol and water, dried in a drying oven and then reused in new reaction.

#### Calculation methods

All DFT calculations were performed using the plane-wave pseudopotential basis set, as implemented in the Vienna *ab initio* simulation package.<sup>52</sup> The ion-electron interactions were treated with the projected augmented wave pseudopotentials,<sup>53</sup> and the generalized gradient approximation parametrized by Perdew, Burke, and Ernzerhof was used to describe the electronic exchange-correlation energy.<sup>54</sup> The outer-shell electrons, i.e., 1s<sup>1</sup> of H, 2s<sup>2</sup>2p<sup>2</sup> of C, 2s<sup>2</sup>2p<sup>4</sup> of O, 4p<sup>6</sup>4d<sup>7</sup>5s<sup>1</sup> of Ru, and 5s<sup>2</sup>5p<sup>6</sup>4f<sup>1</sup>5d<sup>1</sup>6s<sup>2</sup> of Ce were explicitly calculated. An effective Hubbard parameter of 5.0 eV was added for Ce to mitigate the self-interaction errors. The plane-wave basis was expanded up to a cut-off energy of 400 eV. All structures were fully relaxed by the conjugate gradient method until the force component on each atom was less than 0.02 eV/Å, and the convergence criteria of total energy in the

self-consistent field method was set to 10<sup>-5</sup> eV. A typical MOF cluster consisted of Ce, O, and carboxylate groups was adopted to simulate the supporting substrate, and the cluster was put in a cubic box with a side length of 30 Å. The Brillouin zone integration was performed using the  $\Gamma$  point with a Gaussian smearing width of 0.05 eV. The adsorption energy ( $\Delta E_{\text{ads}}$ ) was calculated by:

$$\Delta E_{\text{ads}} = E_{[\text{substrate} + \text{adsorbate}]} - E_{[\text{substrate}]} - E_{[\text{adsorbate}]},$$

where  $E_{[\text{substrate} + \text{adsorbate}]}$  and  $E_{[\text{substrate}]}$  are the DFT energies of the system with and without adsorbate, respectively, and  $E_{[\text{adsorbate}]}$  is the DFT energy for the adsorbate in the gas phase.

#### Conclusions

In summary, taking advantage of the properties UiO-66(Ce), Ru@UiO-66(Ce) catalyst has been designed for dehydrogenation of primary amines to nitriles in water without any hydrogen acceptor and additive. TEM-EDS mapping and HRTEM images reveal that tiny Ru species are highly dispersed on support surface. The Raman and XPS spectra indicate the presence of rich oxygen vacancies and Ru-O-Ce linkages, verifying the existence of Lewis acid-base pairs [Ru-O-Ce-Vö]. Based on experimental and *ab initio* calculation results, the Lewis acid-base pairs in Ru@UiO-66(Ce) can enhance the acceptorless dehydrogenation of primary amines to nitriles by absorption and activation of amine, and the transfer of hydrogen. This chemistry not only provides an efficient catalyst for the acceptorless double dehydrogenation of primary amines, but also elucidates the roles of Lewis acid-base pairs in this transformation which may promote the exploration of new catalysts for the acceptorless dehydrogenation process.

#### Conflicts of interest

There are no conflicts to declare

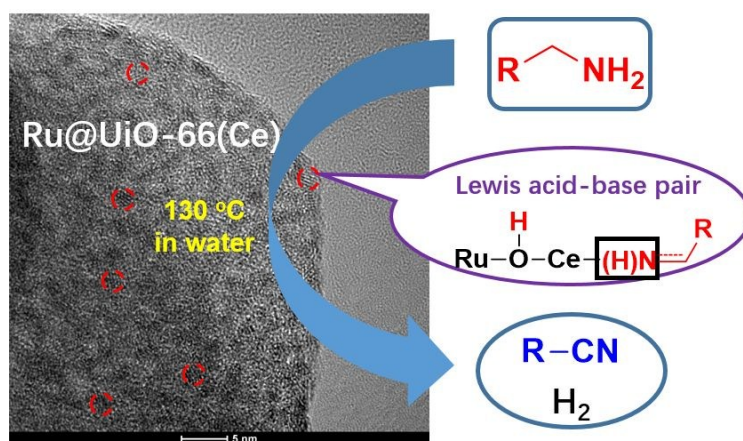
#### Acknowledgements

We gratefully acknowledge Key Laboratory of Biomass Energy and Material, Jiangsu Province (JSBEM201912), Chinese Postdoctoral Science Foundation (2015M571761, 2016T90465) and Jiangsu Provincial Natural Science Foundation of China (BK20160102). This work was a project funded by the Priority Academic Program development of Jiangsu Higher Education Institution.

#### Notes and references

- 1 F. F. Fleming, *Nat. Prod. Rep.*, 1999, **16**, 597-606.
- 2 F. F. Fleming, L. Yao, P. C. Ravikumar, L. Funk, B. C. Shook, *J. Med. Chem.*, 2010, **53**, 7902-7917.
- 3 P. Pollak, G. Romeder, F. Hagedorn, H. P. Gelbke. *Wiley-VCH: Weinheim. Germany.*, 2012.
- 4 C. Song, S. Qu, Y. Tao, Y. Dang, Z. Wang, *ACS Catal.*, 2014, **4**, 2854-2865.

- 5 J. K. Niemeier, R. R. Rothhaar, J. T. Vicenzi, J. A. Werner, *Org. Process Res. Dev.*, 2014, **18**, 410-416.
- 6 K. Yasukawa, R. Hasemi, Y. Asano, *Adv. Synth. Catal.*, 2011, **353**, 2328-2332.
- 7 V. Fassardi, M. Basile, P. Memeo, P. Quadrelli, *Tetrahedron Lett.*, 2017, **58**, 3385-3389.
- 8 J. Kochi, *J. Am. Chem. Soc.*, 1957, **79**, 2942-2948.
- 9 S. Zhang, H. Neumann, M. Beller, *Chem. Eur. J.*, 2018, **24**, 67-70.
- 10 D. Sawant, Y. Wagh, P. Tambade, K. Bhatte, B. Bhanagea, *Adv. Synth. Catal.*, 2011, **353**, 781-787.
- 11 G.-p. Lu, M.-j. Bu, C. Cai, *Synlett*, 2014, **25**, 547-550.
- 12 K. Yamaguchi, H. Fujiwara, Y. Ogasawara, M. Kotani, N. Mizuno, *Angew. Chem. Int. Ed.*, 2007, **46**, 3922-3925.
- 13 K. Ishihara, Y. Furuya, H. Yamamoto, *Angew. Chem. Int. Ed.*, 2002, **41**, 2983-2986.
- 14 A. Falk, A.-L. Goederz, H. Schmalz, *Angew. Chem., Int. Ed.*, 2013, **52**, 1576-1580.
- 15 J. Velcicky, A. Soicke, R. Steiner, H.-G. Schmalz, *J. Am. Chem. Soc.*, 2011, **133**, 6948-6951.
- 16 K. Lambert, J. Bobbitt, S. Eldirany, L. Kissane, R. Sheridan, *Chem. Eur. J.*, 2016, **22**, 5156-5159.
- 17 S. Laulhe, S. S. Gori, M. H.; Nantz, *J. Org. Chem.*, 2012, **77**, 9334-9337.
- 18 S. Kamijo, T. Hoshikawa, M. Inoue, *Org. Lett.*, 2011, **13**, 5928-5931.
- 19 M. Lamani, K. R. Prabhu, *Angew. Chem. Int. Ed.*, 2010, **49**, 6622-6624.
- 20 T. Oishi, K. Yamaguchi, N. Mizuno, *Angew. Chem. Int. Ed.*, 2009, **48**, 6286-6288.
- 21 G.-p. Lu, Y.-m.; Lin, *J. Chem. Res.*, 2014, **38**, 371-374.
- 22 K. Mori, K. Yamaguchi, T. Mizugaki, K. Ebitani, K. Kaneda, *Chem. Commun.*, 2001, **5**, 461-462.
- 23 Y. Shen, Y. Zhou, L. Jiang, G.; Ding, G. Luo, Z.; Zhang, *Tetrahedron*, 2018, **74**, 4266-4271.
- 24 K. C. Nicolaou, C. J. N. Mathison, *Angew. Chem. Int. Ed.*, 2005, **44**, 5992-5997.
- 25 C. Tao, F. Liu, Y. Zhu, W. Liu, Z. Cao, *Org. Biomol. Chem.*, 2013, **11**, 3349-3354.
- 26 R. H. Crabtree, *ACS Sustain. Chem. Eng.*, 2017, **5**, 4491-4498.
- 27 I. Dutta, S.; Yadav, A.; Sarbajna, S. De, M. Ischer, *J. Am. Chem. Soc.*, 2018, **140**, 8662-8666.
- 28 K. N. Tseng, A. M. Rizzi, N. K. Szymczak, *J. Am. Chem. Soc.*, 2013, **135**, 16352-16355.
- 29 M. Grellier, S. Sabo-Etienne, *Dalton Trans.*, 2014, **43**, 6283-6286.
- 30 D. Ventura-Espinosa, A. Marza-Beltran, J. A.; Mata, *Chem. Eur. J.*, 2016, **22**, 17758-17766.
- 31 C. Gunanathan, D. Milstein, *Science*, 2013, **341**, 1229712.
- 32 P. T. Anastas, J. C. Warner, *Green Chemistry: Theory and Practice*. Oxford University Press, Oxford, UK, 1998.
- 33 P. T. Anastas, T. Williamson, *Green Chemistry, Frontiers in Benign Chemical Synthesis and Process*. Oxford University Press, Oxford, UK, 1998.
- 34 C. U. Fischer, K. Hungerbuhler, *Green Chem.*, 2007, **9**, 927-934.
- 35 Y. Wang, J. Zhang, H. Chen, Z. Zhang, C. Zhang, M. Li, F. Wang, *Green Chem.*, 2017, **19**, 88-92.
- 36 J. An, Y. Wang, J. Lu, J. Zhang, Z. Zhang, S. Xu, *J. Am. Chem. Soc.*, 2018, **140**, 4172-4181.
- 37 J. An, Y. Wang, Z. Zhang, Z. Zhao, J. Zhang, F. Wang, *Angew. Chem. Int. Ed.*, 2018, **57**, 12308-12312.
- 38 D. H. Nguyen, X. Trivelli, F. Capet, Y. Swesi, *ACS Catal.*, 2018, **8**, 4719-4734.
- 39 Z. Hu, D. Zhao, *Dalton Trans.*, 2015, **44**, 19018-19040.
- 40 M. Lammert, M. T. Wharmby, S. Smolders, B. Bueken, A. Lieb, K. A. Lomachenko, D. D. Vos, N. Stock, *Chem. Commun.*, 2015, **51**, 12578-12581.
- 41 X. P. Wu, L. Gagliardi, D. G. Truhlar, *J. Am. Chem. Soc.*, 2018, **140**, 7904-7912. View Article Online  
DOI: 10.1039/C9GC02181G
- 42 Z. Hu, Z. Wang, Y. Guo, L. Wang, F. Guo, J. Zhang, W. Zhan, *Environ. Sci. Technol.*, 2018, **52**, 9531-9541.
- 43 T. Sakpal, L. Lefferts, *J. Catal.*, 2018, **367**, 171-180.
- 44 F. Wang, S. He, H. Chen, B. Wang, L. Zheng, M. Wei, D. Evans, D. X. Duan, *J. Am. Chem. Soc.*, 2016, **138**, 6298-6305.
- 45 X. Wang, X. Peng, Y. Zhang, J. Ni, C. Au, L. Jiang, *Inorg. Chem. Front.*, 2019, **6**, 396-406.
- 46 J. Bokal, M. Zawadzki, P. Kraszkiewicz, K. Adamska, *Appl. Catal. A-Gen.*, 2018, **549**, 161-169.
- 47 Q. Yang, Q. Xu, H. L. Jiang, *Chem. Soc. Rev.*, 2017, **46**, 4774-4808.
- 48 H. Ren, C. Li, D. Yin, J. Liu, C. Liang, *RSC Adv.*, 2016, **6**, 85659-85665.
- 49 D. Jiang, G.; Fang, Y. Tong, X. Wu, Y. Wang, D. Hong, *ACS Catal.*, 2018, **8**, 11973-11978.
- 50 J.-W. Zhang, D.-D. Li, G.-P. Lu, T.; Deng, C. Cai, *ChemCatChem*, 2018, **10**, 4258-4263.
- 51 J.-W. Zhang, D.-D.; Li, G.-P. Lu, T.; Deng, C. Cai, *ChemCatChem* 2018, **10**, 4966-4972.
- 52 G. Kresse, J. Furthmüller, *Phys. Rev. B*, 1996, **54**, 11169-11186.
- 53 P. E. Blochl, *Phys. Rev. B*, 1994, **50**, 17953-17979.
- 54 J. P. Perdew, K. Burke, M. Ernzerhof, *Phys. Rev. Lett.*, 1996, **77**, 3865-3868.
- 55 D. Wang, Y. Li, *Adv. Mater.*, 2011, **23**, 1044-1060.
- 56 K. D. Gilroy, A. Ruditskiy, H. C. Peng, D. Qin, Y. Xia, *Chem. Rev.*, 2016, **116**, 10414-10472.
- 57 M. Sankar, N. Dimitratos, P. J. Miedziak, P. P. Wells, C. J. Kiely, G. J.; Hutchings, *Chem. Soc. Rev.*, 2012, **41**, 8099-8139.
- 58 F. Wang, S. He, H. Chen, B. Wang, L. Zheng, M. Wei, *J. Am. Chem. Soc.*, 2016, **138**, 6298-6305.
- 59 G. Ou, Y. Xu, B. Wen, R. Lin, B. Ge, Y. Tang, Y. Liang, C. Yang, K. Huang, D. Zu, R. Yu, W. Chen, J. Li, H. Wu, L. M. Liu, Y, *Nat. Commun.*, 2018, **9**, 1302.
- 60 L. Wang, J. Zhang, G. Wang, W. Zhang, C. Wang, C. Bian, F. S. Xiao, *Chem. Commun.* 2017, **53**, 2681-2684.
- 61 T. Sakpal, L. Lefferts, *J. Catal.*, 2018, **367**, 171-180.
- 62 Y. Liu, Y. Wu, Z. Akhtamberdinova, X. Chen, G. Jiang, D. Liu, *ChemCatChem*, 2018, **10**, 4689-4698.
- 63 T. Rodrigues, A. Moura, F. Silva, E. Candido, A. Silva, D. Oliveira, J. Quiroz, P. Camargo, V. Bergamaschi, J. Ferreira, M. Linar, F. Fonseca, *Fuel*, 2019, **237**, 1244-1253.
- 64 M. Kumar, J.-H. Yun, V. Bhatt, B. Singh, J. Kim, J.-S. Kim, *Electrochim. Acta.*, 2018, **284**, 709-720.
- 65 Z. Luo, Z. Zheng, L. Li, Y.-T. Cui, C. Zhao, *ACS Catal.*, 2017, **7**, 8304-8313.
- 66 J.-W. Zhang, D.-D. Li, G.-P. Lu, T. Deng, C. Cai, *ChemCatChem*, 2018, **10**, 4966-4972.
- 67 C. Zhu, T. Ding, W. Gao, K. Ma, Y. Tian, X. Li, *Int. J. Hydrog. Energy*, 2017, **42**, 17457-17465.
- 68 The solvation effects of water may reduce about 0.3 eV of the adsorption energy for hydrogen on Ce, so the adsorption energy for hydrogen on Ce (site 1) should be less than zero in the actual situation. J. K. Nørskov, J. Rossmeisl, A. Logadottir, L. Lindqvist, J. R. Kitchin, T. Bligaard, H. Jónsson, *J. Phys. Chem. B*, 2004, **108**, 17886-17892.



View Article Online  
DOI: 10.1039/C9GC02181G